ChemPubSoc Europe

DOI: 10.1002/open.201800268

Open Access ChemistryOPEN Full Papers

# Highly Active Catalysis of Cobalt Tetrakis (pentafluorophenyl)porphyrin Promoted by Chitosan for Cyclohexane Oxidation in Response-Surface-Methodology-Optimized Reaction Conditions

Lin-Qiang Mo,[a] Xian-Fei Huang,*[b] Guan Huang,*[a] Guang-Ping Yuan,[a] and Su-Juan Wei[a]

We aimed at elevating catalytic performances of cobalt tetrakis (pentafluorophenyl)porphyrin (Co TPFPP) through axial coordination, nanocavities, and covalently grafting action. The Co TPFPP was immobilized onto nanoporous and nonporous chitosan, forming Co TPFPP/np- and nonp-CTS catalysts, respectively. The catalysts were characterized by various spectroscopic techniques. The catalytic performances of these catalysts for cyclohexane oxidation under response-surface-methodology-optimized oxidation reaction conditions were estimated and compared. Co TPFPP/np-CTS was an excellent catalyst at aspect of catalytic activity, exhibiting the considerable potential reusability, 24.2 mol% yields (KA oil : cyclohexanone and cyclohexanol) in average, and total turnover frequencies (TOFs) of $3.25\times10^6$ $h^{-1}$. This is attributed to the structural characteristics of the Co TPFPP/np-CTS catalyst: the cobalt porphyrin molecules could be highly scattered on CTS, forming the independent active sites, and were not leached. The axial coordination exerted the most important effect on the catalytic activity, and the covalent grafting action had a decisive effect on the increase of the total TOFs and on the reusability of the catalyst.

## 1. Introduction

Cytochrome P450 enzyme has a special structure with an important acid group, a key axial cysteine ligand and a natural cavity. This natural structure makes the enzyme, its related artificial enzyme and biomimetic catalyst having excellent functionality and becoming an important catalyst used for substrate oxidation.[1–4] Duplication of the core structure and part functions of the enzyme using immobilized metalloporphyrin systems is of tremendous interest in order to improve the performance (activity and reusability) of metalloporphyrins.[3–10] The effect of N-bases axial coordination on the catalytic activity of metalloporphyrin has been studied about 20–30 years ago, and some achievements were obtained.[3,11–13] At present, some new studies on the effect of the axial ligand on catalytic activity of metalloporphyrins[3,8, 9] suggested that, the enhanced catalytic activity was attributed to the increased electron donation ability and favoring the formation of the ferryl-oxo species, and that the "push" effect prevails over the "pull" effect.[8] The studies suggested that, the coordination of the axial ligand made $O_2$ more activated than the free $O_2$, and triggered the catalytic oxidation processes. Finally, it has been proposed that,the larger the electron cloud density of the bound nitrogen atom of the axial ligand was, the more active the binding $O_2$ became.[14]Christoforidis[8] also gave another convinced evidence that deprotonation of the axial imidazole led to the increased ability to donate electrons to the central metal. Jiang[15] has reported that H-bonding (Por-N···H–MeIM) affected the binding energy (BE) of the Mn core electron in Mn-TAPP@ZIF-8 and then promoted its catalytic activity; Green and co-workers[16] have revealed that, H-bonding could shorten the Fe–S bond in P450-I for greater electron donation into the ferryl π* orbitals, weakening the Fe=O bond, resulting in the higher catalytic activity. However, there is still a challenge of quantitatively characterizing the strength of the coordination of these ligands to the metalloporphyrins.[13] Because the coordination strength is closely related to the catalytic activity.

The successful researches and the challenge above inspired us to use the various metalloporphyrins immobilized on the different carries as catalysts for investigating how the axial coordination enhanced their catalytic activities.[17,18] We have not only found that, a sulfur- or nitrogen-containing ligand in the corresponding support could affect the binding energy of the metal center in metalloporphyrins and then promote the

[a] Dr. L.-Q. Mo, G. Huang, G.-P. Yuan, S.-J. Wei
School of Chemistry and Chemical Engineering
Guangxi University
530004,Nanning, Guangxi, P.R.China
E-mail: huangg66@126.com
[b] X.-F. Huang
School ofComputerandElectronicInformation
Guangxi University
530004,Nanning, Guangxi, P.R.China
E-mail: huang1023oblivion@outlook.com

Supporting information for this article is available on the WWW under https://doi.org/10.1002/open.201800268

catalytic activity of the immobilized metalloporphyrin, but also found that, each of the catalysts (Co TCPP/ZnS, or Fe TPPS/pd-CTS) could be only reused 2 times respectively for the oxidation of cyclohexane.[17,18] The experiences above[8,14,17,18]encouraged us to consider the stability issue of immobilized metalloporphyrin catalyst: the hexane diacid produced in the cyclohexane oxidation system, will affect the activity and reusability of the immobilized metalloporphyrin catalysts. This is a newly-discovered issue for preparing an immobilized metalloporphyrin catalyst with high catalytic activity and multiple reusability. This promoted us to graft metalloporphyrin onto support, ensuring its multiple reusability.

The porous catalyst materials could be unified the best characters of homogeneous and heterogeneous catalysts[19] and they could also promote the substrate conversion, and the recycling ability.[20,21]Interestingly, powder chitosan (pd-CTS) can be chemically and physically modified into nano- and non-porous chitosan (np- and nonp-CTS), which might be used to immobilize metalloporphyrins as various catalysts. These drove us to further investigate the comprehensive effect of covalently grafting-action, axial coordination, and nanocavity of chitosan on the catalytic performance (activity and reusability) of CTS-immobilized metalloporphyrin.

As the best of our knowledge, recently four decades, using molecular oxygen ($O_2$) as oxidant, and metalloporphyrin as catalyst to mimic the core structure and part functions of cytochrome P-450 enzyme for hydroxylation of hydrocarbon, there were at least two systems: one was added reductant ($NaBH_4$),[22] its non-radical-reaction was similar to Gif chemistry,[23,24] and another did not need $NaBH_4$,[22] both were conducted in solvent and at room temperature. Lyons and Lindsay Smith successfully used the latter system at 80–100 °C, and considered that the oxidation mechanism was a typical free radical reaction.[25,26] For further avoiding use of any solvents and reductants (toxic or not), some studies have been efficiently made on hydrocarbon oxidation at relatively high temperature catalyzed by metalloporphyrin and supported ones.[20,27,28] Based on the consideration of practical application in green chemical industry, the improved Lyon system was preferred for us.[10,17,18]

We aimed at elevating catalytic performances (activity and reusability) of cobalt tetrakis(pentafluorophenyl)porphyrin (Co TPFPP), and report in here that, cobalt tetrakis(pentafluorophenyl)porphyrin was covalently and coordinately bound to np- and nonp-CTS, forming new catalysts, Co TPFPP/np- or nonp-CTS. Both catalysts were used for cyclohexane oxidation under optimized reaction conditions via a response surface methodology (RSM). The catalytic performances (activity and reusability) promoted by axial coordination, covalently grafting, and nanocavity of chitosan were investigated. RSM is a very popular-used statistical technique,[29,30] which fits to be used in research into complex variable processes. It could help us obtaining optimized reaction conditions and high catalytic performances of Co TPFPP/np-CTS.Main Text Paragraph.

## 2. Results and Discussion

### 2.1. Characterization of the Grafted Catalyst Materials

When Co TPFPP was grafted to the np-CTS yellow microballs, the appearance of np-CTS changed into yellowish brown, forming Co TPFPP/np-CTS microballs. The cobalt porphyrin was grafted to the red nonp-CTS microballs, brown Co TPFPP/nonp-CTS microballs were obtained. The color changes were caused by the grafted cobalt porphyrin to chitosan. Some differences will be found after carefully comparing the original SEM micrographs of np-CTS and Co TPFPP/np-CTS : the texture structure of Co TPFPP/np-CTS, in some spots, showed a more contracted texture-threads (Figure 1). This was caused by covalently grafting Co TPFPP molecules to np-CTS (Scheme 1).

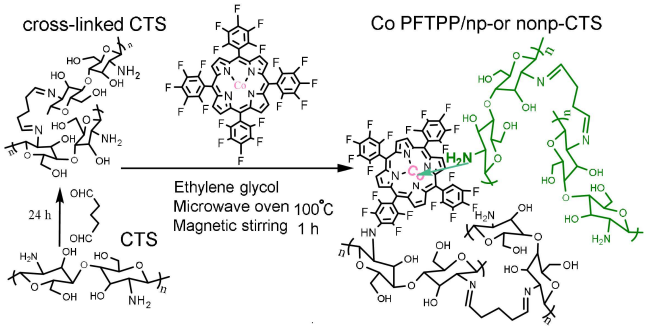


**Scheme 1.** Synthetic route for the preparation of Co TPFPP/np- or nonp-CTS.

They were highlyscattered on np-CTS (Figure 1 STEM), one by one, immobilized, and acted as the independently active site. The STEM micrographs of Co TPFPP/np-CTS and Co TPFPP/nonp-CTS also show that, Co TPFPPs were highly dispersed onto np-CTS and nonp-CTS. Because the diameters of the black spots in their STEM images, were approximately 2–3 nm. The dispersion can be also further proved via the EDS elemental mapping of the Co ions, which were highly scattered (Figure 1 Co). Compared with the np-CTS and Co TPFPP/np-CTS, the nonp-CTS and Co TPFPP/nonp-CTS possessed more contracted structure (SEM micrograph, Figure 1) caused by drying in vacuum at 60 °C for 8 hours. This also resulted in a difficulty of detecting their $S_{BET}$ data in the same way.

The $N_2$ adsorption/desorption isotherm and BJH pore-size distribution curves of np-CTS and Co TPFPP/np-CTS indicate that the materials consisted of micropore, mesopore, and macropore, but mainly of approximately 2–100 nm pore diameter (Figure 2 and Table 1). These are heralding that, the active sites of Co TPFPP/np-CTS have more chances to touch reaction substrates, relative to those of Co TPFPP/nonp-CTS.

Immobilizations of Co TPFPP to np-/nonp-CTS were further verified by UV-Vis spectra analyses (Figure 3). For the Co TPFPP UV-Vis spectra, its Soret peak at 404 nm was red-shifted to the Soret peak of Co TPFPP/np-CTS at 410 nm, and that of Co TPFPP/nonp-CTS at 428 nm. The Soret peak red-shift confirmed the coordination between Co TPFPP and np-CTS;[31,32] alterna-

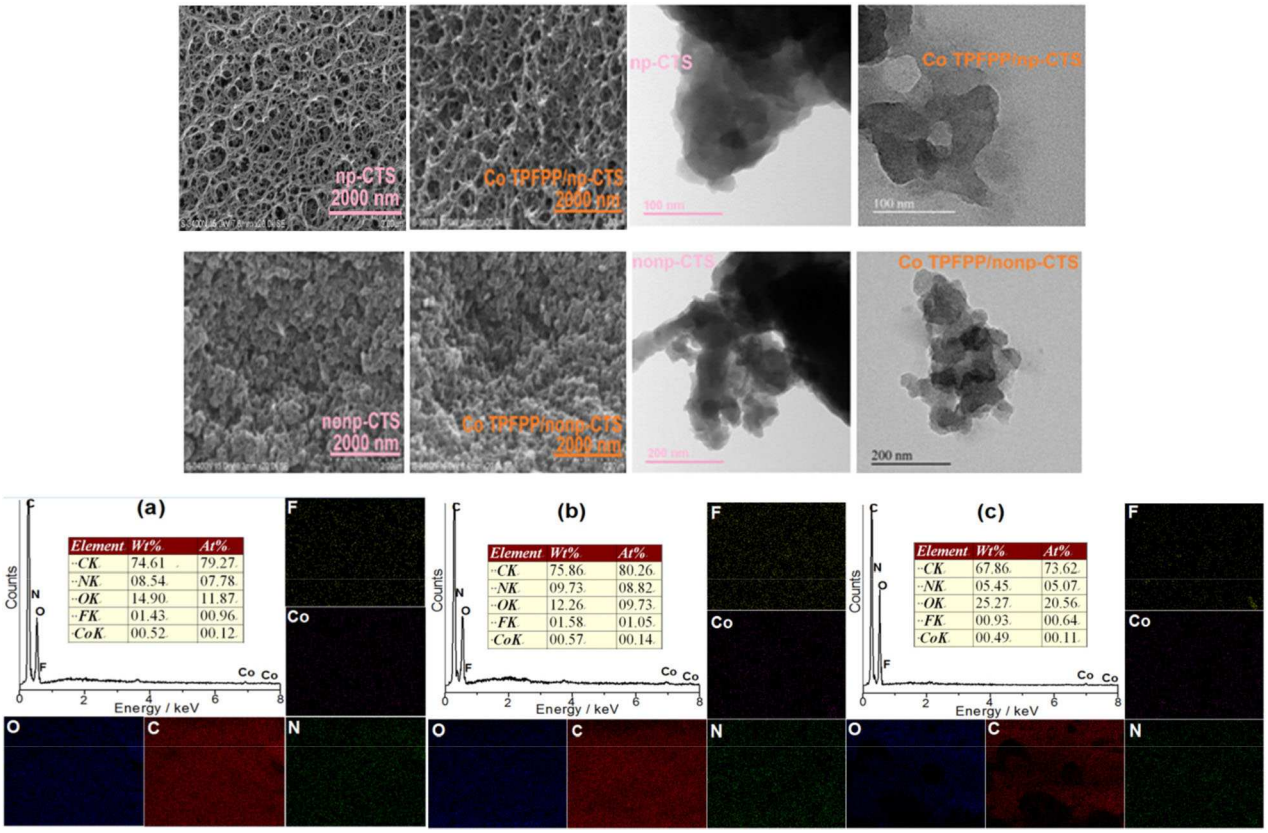


**Figure 1.** SEM and STEM images of np-CTS, nonp-CTS, Co TPFPP/np-CTS, and Co TPFPP/nonp-CTS; EDS images of Co TPFPP/np-CTS (a), Co TPFPP/nonp-CTS (b), and Co TPFPP/np-CTS recovered after 5$^{th}$ run of recycle (c),inserts are the EDS elemental mapping of Co, N, C, O, and F.

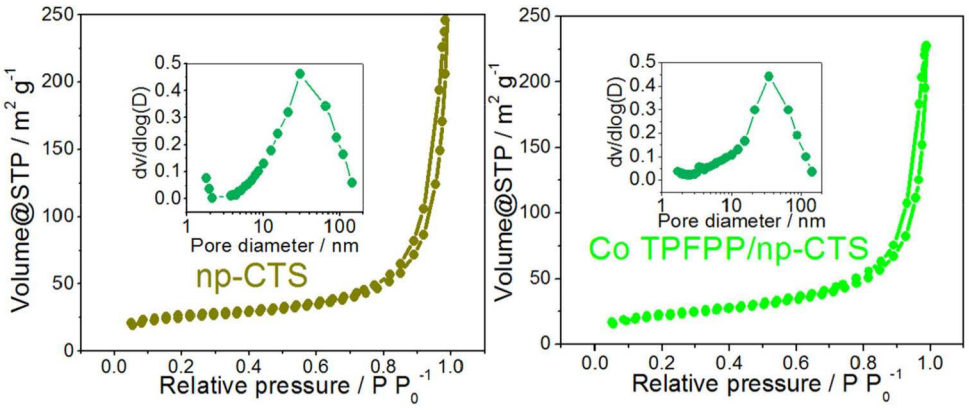


**Figure 2.** The $N_2$ adsorption/desorption isotherm and BJH pore-size distribution curves of np-CTS (left) and Co TPFPP/np-CTS (right).

**Table 1.** Physical properties of np (nonp)-CTS and Co TPFPP/np (nonp)-CTS.

| Materials | Surface area [$m^2 g^{-1}$] | Pore diameter [nm] |
|---|---|---|
| np-CTS | 89.5 | 20.6 |
| Co TPFPP/np-CTS | 77.2 | 17.7 |
| nonp-CTS | 2.5 | – |
| Co TPFPP/nonp-CTS | 2.1 | – |

tively, Co TPFPP grafted to np-CTS became less planar.[33] This preliminarily indicates that Co TPFPPs have been grafted to np- or nonp-CTS, forming the corresponding compounds, Co TPFPP/np- or nonp-CTS. Grafting and coordinating of cobalt porphyrin onto CTS could be proved by their FTIR spectra (Figure 4). Because np- or nonp-CTS was obtained by cross-linking CTS with glutaraldehyde, the amide II absorption peak at 1597 $cm^{-1}$and the -$NH_2$ group peak at 3373 $cm^{-1}$ in CTS[34] were respectively changed to a short peak at 1569~1597 $cm^{-1}$and a narrow peak at 3415 $cm^{-1}$ in np-CTS (Herein,

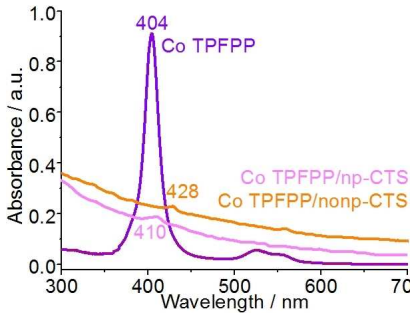


**Figure 3.** UV/Vis spectra for the DCM solutions of Co TPFPP ($\varepsilon = 3.40\times10^5$ L·mol$^{-1}$·cm$^{-1}$), and for DCM suspensions of Co TPFPP/np-CTS ($\varepsilon = 8.27\times10^3$ mol$^{-1}$·cm$^{-1}$), Co TPFPP/nonp-CTS($\varepsilon = 8.28\times10^3$ mol$^{-1}$·cm$^{-1}$).

the disturbance from the vibration peaks of hydroxyl groups in CTS should be considered). These showed a stronger peak of hydroxyl group at 3415 cm$^{-1}$ in np-CTS than that in CTS, while, a weaker peak of amino group at 3317 cm$^{-1}$ in np-CTS than that in nonp-CTS. The reason is that an imine bond, C=N, was formed between CTS and glutaraldehyde, a small shoulder peak was present at ~1658 cm$^{-1}$(Figure 4).[35] Nonp-CTSshowed similar peaks with those of np-CTS, there were slight differences between them for the two peaks at 3415 cm$^{-1}$ and at 3317 cm$^{-1}$. This is because when they were formed, nonp-CTS lost more moisture than did np-CTS. For covalently grafting Co TPFPP to np-CTSvia nucleophilic substitution of para-F on a benzene ring in Co TPFPP using an amino group (-NH$_2$) of np-CTS, the key evidence is that, the amino peak of np-CTS at $<$3415 cm$^{-1}$ shifted to the amino peak of Co TPFPP/np-CTS at $<$3404 cm$^{-1}$. These results were similar to those reported in reference.[36] A mechanic mixture of Co TPFPP with np-CTS, Co TPFPP + np-CTS, had no the similar change of spectroscopic characteristics (Figure 4). The presence of a peak at 521 cm$^{-1}$ for Co TPFPP/np-CTS indicates the formation of a Co–N$_{(axial)}$ coordination bond between Co TPFPP and np-CTS (Figure 4).[37] Because the characteristic absorption of Co–N$_{(equatorial)}$ bond in Co TPFPP appeared at 1008 cm$^{-1}$.[32] Therefore, we suggest that Co TPFPP/np-CTS possessed the structure in Scheme 1. Like np-CTS, nonp-CTS was also obtained by cross-linking CTS with glutaraldehyde but by drying in the different way above: the water adsorbed physically on hydroxyl, carbonyl and amino groups of CTS were removed, and hydrogen-bonds were somewhat destroyed.[38] This resulted in an amide II absorption peak being present at 1569 cm$^{-1}$, and an –NH$_2$ group peak being present at 3317 cm$^{-1}$. A small shoulder peak at ~1668 cm$^{-1}$ was found and ascribed to be an imine bond (C=N). Covalently grafting Co TPFPP to nonp-CTS via the

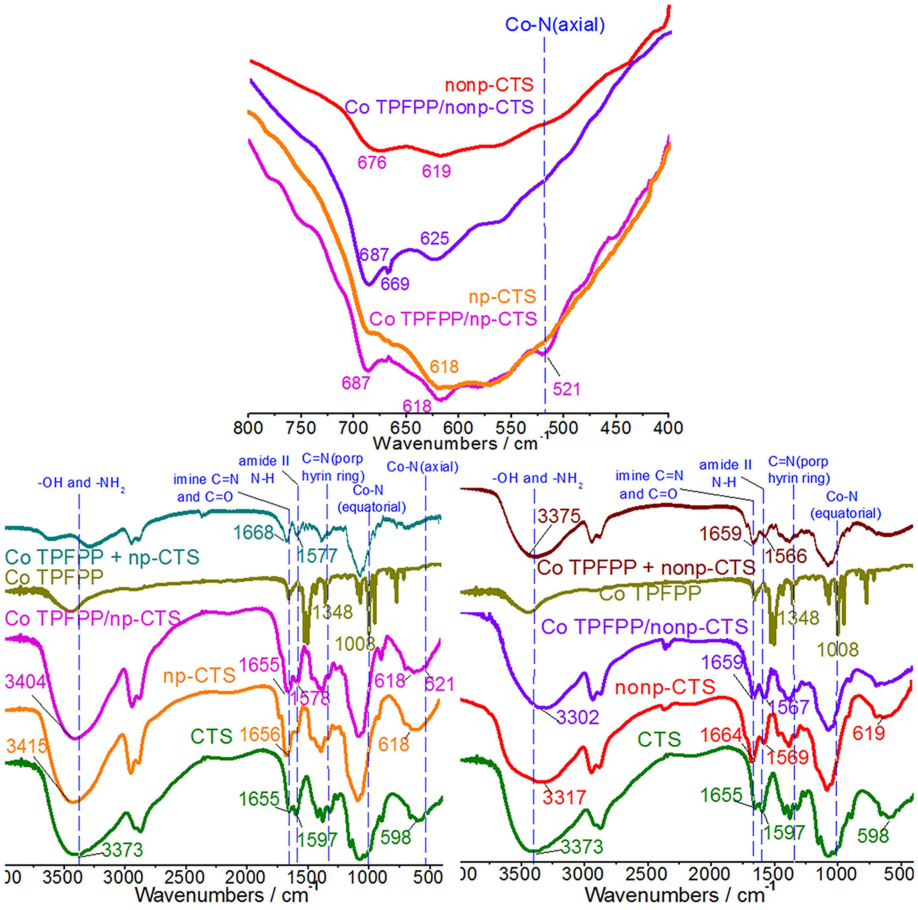


**Figure 4.** FTIR spectra for np(or nonp)-CTS and Co TPFPP/np(or nonp)-CTS with an effective frequency range of 800–400 cm$^{-1}$ (top), FTIR spectra for CTS, np-CTS, Co TPFPP, Co TPFPP/np-CTS, np-CTS + Co TPFPP (left), and CTS, nonp-CTS, Co TPFPP, Co TPFPP/nonp-CTS, nonp-CTS + Co TPFPP (right) with an effective frequency range of 4000–400 cm$^{-1}$.

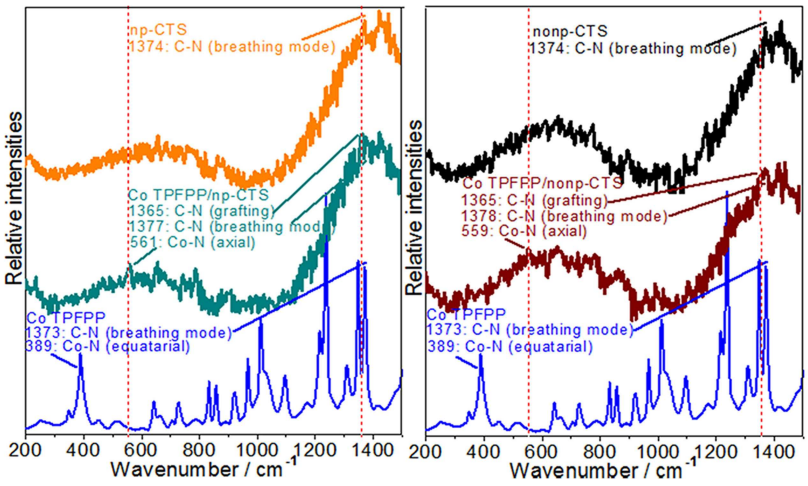


**Figure 5.** Resonance Raman spectra of np-CTS, Co TPFPP, Co TPFPP/np-CTS (left), and nonp-CTS, Co TPFPP, Co TPFPP/nonp-CTS (right), pulsed excitation at 325 nm.

**Table 2.** The binding energy of the key elements in CoTPFPP/np (nonp-)-CTS, Co TPFPP, and np (nonp-)-CTS.

| XPS spectra | Existing form ofthe key elements | Binding Energy [eV] Co TPFPP/np-CTS (Co TPFPP/nonp-CTS) | Co TPFPP | np-CTS (nonp-CTS) | dBE [eV] |
|---|---|---|---|---|---|
| Co2p | *Co*–N | 804.5(803.9) | 795.9 | – | 8.6(8.0) |
| | | 784.2(784.2) | 780.6 | – | 3.6(3.6) |
| N 1s | *N*–C=[*N*=C] | 399.6(399.2) | 399.1 | – | 0.5(0.1) |
| | *N*–Co | 399.4(399.0) | 399.0 | – | 0.4(0.0) |
| | $NH_2$–$C_{sp3}$ | 399.2(398.6) | – | 398.1(399.6) | 1.1(-1.0) |
| | *N*=$C_{sp2}$ | 401.9(401.2) | – | 400.9(400.1) | 1.0(1.1) |
| | *N*H–C=O | 402.5(402.7) | – | 402.5(402.8) | 0.0(-0.1) |
| C1s | C=C–F | 284.8(285.4) | 287.9 | — | |
| | C=C–NH | 284.7(284.6) | – | | -3.2(-3.3) |

nucleophilic substitution reaction above could be proved by thered-shift of the peaks at 3317 $cm^{-1}$ in nonp-CTS to a peak at 3302 $cm^{-1}$ in Co TPFPP/nonp-CTS.[39] However, there was maybe a Co–N weak axial coordination bond between Co TPFPP and nonp-CTS, which was obscure. For further making clear the two issues: covalently grafting and axially coordinating of Co TPFPP to np-CTS and nonp- CTS, their Raman spectra were compared in Figure 5. The resonance Raman (RR) spectra of Co TPFPP show that, the peak at 1373 $cm^{-1}$ was attributed to a C–N bond stretching vibration;[40–42] while the peak at 389 $cm^{-1}$was assigned to a Co–N bond stretching vibration.[44] After Co TPFPP was grafted and coordinated onto np-CTS and nonp-CTS, forming CoTPFPP/np-CTS and Co TPFPP/nonp-CTS, their axially coordinated newly bonds (Co–N) respectively were present at 561 $cm^{-1}$ and 559 $cm^{-1}$,[44,45] and their covalently grafted newly bonds (C–N) were present at 1365 $cm^{-1}$ (Figure 5).

The axial coordination and covalently grafting of Co TPFPP to np-CTS and nonp-CTS changed the electron cloud densities of all elements, especially those of the Co metal and elements (Cl, N) most proximal to the cobalt ion in Co TPFPP. These changes can be seen and assigned in Table 2 and Figure 6.[17,18] The nucleophilic substitution of the 4-F atom on the benzene ring of Co TPFPP by the $NH_2$–C unit in np-CTS and nonp-CTS took place. That is, the covalently grafting of the nitrogen atom of the amino group (–$NH_2$) in np-CTS and nonp-CTS to the 4-C atom on the benzene ring of Co TPFPP; the 4-C atoms of the C=C–F unit in Co TPFPP were changed to the 4-C atoms of the C=C–NH unit in Co TPFPP/np-CTS and Co TPFPP/nonp-CTS. Therefore, the binding energy (287.9 eV) of the 4-C atoms in theC=C–F unit of CoTPFPP respectively decreased to 284.7 eV of the 4-C atoms in the C=C–NH unit of CoTPFPP/np-CTS, and 284.6 eV of the 4-C atoms in the C=C–NH unit of Co TPFPP/nonp-CTS (Table 2). The two dBE values (−3.2 vs−3.3) of the both catalysts indicate that, Co TPFPPs were tightly grafted to np-CTS and nonp-CTS via a very similarly strong C–N bond.

Axially coordinating the amino group (–$NH_2$) of np-CTS and nonp-CTS to the cobalt ion of Co TPFPP, resulted in that, the nitrogen atoms of the $NH_2$–$Csp^3$ unit in np-CTS and nonp-CTS were changed into the nitrogen atoms of the $NH_2$–$Csp^3$ unit in Co TPFPP/np-CTS and Co TPFPP/nonp-CTS, and the dBE values were 1.1 eV and−1.0 eV, respectively (Table 2). The dBE difference shows that the coordination intensity of np-CTS was stronger than that of nonp-CTS.

Afterwards, based on the very similarly covalently- grafting strength above, the stronger axial coordination probably resulted in that, the equatorial nitrogen coordination (dBEs: 0.5 and 0.4 eV) to cobalt ion of Co TPFPP/np-CTS was stronger (relative to the coordination in Co TPFPP/nonp-CTS (dBEs: 0.1 and 0.0 eV)), and that, the dBE (8.6 eV) of cobalt ion of Co

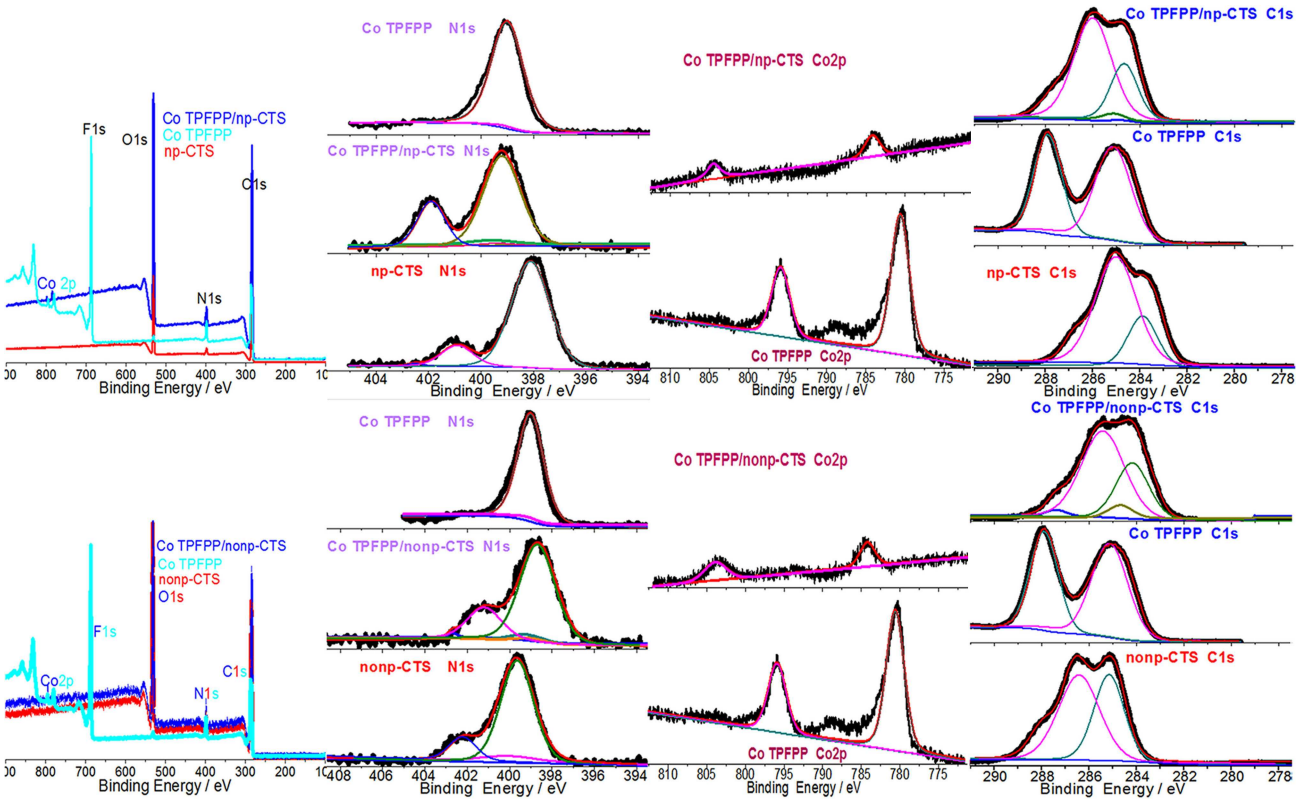


**Figure 6.** X-ray photoelectron spectra and main spectral bands based on the BE of the Co, N, and C elements for np-CTS, Co TPFPP, Co TPFPP/np-CTS (top), and nonp-CTS, Co TPFPP,and Co TPFPP/nonp-CTS (bottom).

TPFPP/np-CTS was larger than that (8.0 eV) of Co TPFPP/nonp-CTS (Table 2). This means that,the cobalt ion of Co TPFPP/np-CTS carried more positive charges used for binding and activating $O_2$,showing its highest catalytic activity.

### 2.2. Catalysis of the Grafted Catalyst Materials for Cyclohexane Oxidation

In order to investigate the effects of the axial coordination, the covalently grafting and the nano-cavity on the catalytic activities of Co TPFPP/np-CTS, we used the three catalysts (Co TPFPP/np-CTS, Co TPFPP/nonp-CTS, and Co TPFPP) to catalyze oxidation of cyclohexane, and compared the catalytic activities of these catalysts under RSM –optimized oxidation reaction conditions (oxidation temperatures, $O_2$ pressure, and amount of catalyst) (see Figure 7 and Table 3).

First, the TOFs ( or TON) obtained from the cyclohexane oxidation over CoTPFPP/np-CTS were higher than those of Co TPFPP after 2-hours reaction time. At the optimal reaction time of ~3.5 hours, the catalytic activity of Co TPFPP/np-CTS was approximately 1.5 times as much as that of Co TPFPP. This indicates that, primarily, the axial coordination (dBE = 1.1 eV) of the N atoms to the cobalt ion of Co TPFPP, and secondlythe nano-cavity of CTS improved the catalytic activity of cobalt porphyrin. This is becausethat, (1) the electron cloud density of the bound nitrogen atom of the axial ligand (–$NH_2$) in Co TPFPP/np-CTS decreased. It indicated the strong coordination of amino to cobalt porphyrin, and resulted in more effect to activate $O_2$,[8,14] just as the XPS-analyzed result above. (2) the nano-cavity of CTS benefited to cyclohexane and $O_2$ accessing the active sites. Indeed, this was a synergism of the two factors, especially the coordination, elevated the catalytic activity of Co TPFPP/np-CTS and resulted in always increasing of TOF until 3.5 h. After 3.5-h reaction time, the TOFs (or TON)obtained from

**Table 3.** Comparison of catalytic performances of related catalysts under the best RSM-optimized reaction conditions.[a]

| Catalyst | Run | TOF ($\times 10^5$ $h^{-1}$) | TON ($\times 10^5$) | Yield [%] | Selectivity [%] |
|---|---|---|---|---|---|
| Co TPFPP/np-CTS | 1 | 2.5 | 8.7 | 26.4 | 65.0 |
| | 2 | 3.7 | 12.9 | 25.9 | 64.1 |
| | 3 | 6.6 | 23.1 | 25.2 | 62.9 |
| | 4 | 9.3 | 32.4 | 23.0 | 61.5 |
| | 5[b] | 10.4 | 36.5 | 20.7 | 60.3 |
| | **Average** | **6.5** | **22.7** | **24.2** | **62.8** |
| Co TPFPP | 1 | 1.6 | 5.6 | 18.5 | 72.0 |
| Co TPFPP + CTS | 1 | 1.6 | 5.7 | 18.7 | 70.4 |
| Co TPFPP/nonp-CTS | 1 | 1.3 | 4.4 | 13.9 | 69.9 |
| | 2 | 1.7 | 6.0 | 13.4 | 69.3 |
| | 3 | 2.4 | 8.3 | 11.6 | 69.1 |
| | 4 | 3.6 | 12.5 | 11.0 | 68.4 |
| | 5 | 4.9 | 17.2 | 10.7 | 68.0 |
| | **Average** | **2.8** | **9.7** | **12.1** | **68.9** |

[a] 200 mLcyclohexane, 165.14 °C, 0.8 MPa, 0.98 mg Co TPFPP, oxygen flow rate of 0.03 $m^3$/h, and reaction time of 3.5 hours. TOF: turnover frequency; TON: turnover number. [b] Its reuse was not stopped here.

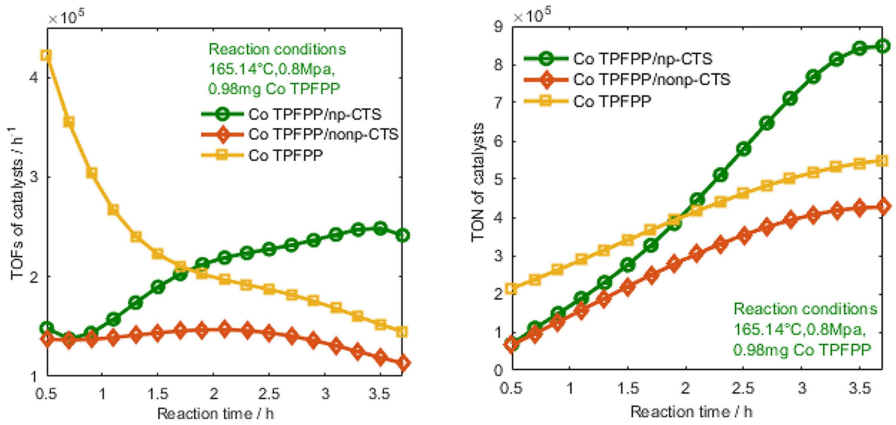


**Figure 7.** Changes in the TOF (left) and TON (right) of the catalysts with reaction time, under cyclohexane oxidation reaction conditions optimized by RSM. Reaction conditions: $O_2$ flow rate = 0.03 $m^3 \cdot h^{-1}$ and 3.5 hours reaction time.

the cyclohexane oxidation over Co TPFPP/np-CTS showed dropping down, due mainly to the more and more effect of the produced more hexane diacid on the catalytic activity of the catalyst. The nitrogen atom of the axial ligand (–$NH_2$) in Co TPFPP/np-CTS was protonated, this action was similar to the nitrogen atom situation of the axial imidazole as-reported.[8,14] Because the cobalt content of the fifth recovered Co TPFPP/np-CTS (as well as on its surface, see Figure 1 (a) versus (c)) was not changed obviously by ICP-OES analyses.

Second, the TOFs ( or TON) obtained from the cyclohexane oxidation over Co TPFPP/np-CTS were higher than those over Co TPFPP/nonp-CTS after 0.5-hour reaction time. It shows that the axial coordination (dBE = 1.1 eV) primarily promoted the increment of the TOFs (or TON), enhancing the catalytic activity of Co TPFPP. Next, under the same grafting action, due to coordination, and nano-cavity, the double actions still played an important role in enhancing its catalytic activity, made Co TPFPP/np-CTS more activating $O_2$ than Co TPFPP/nonp-CTS in reuse, and elevating TOF (or TON) in each run. However, such increasing activity could result in peroxidation of KA oil into by-products and then dropping the selectivity. Obviously, the selectivity decrements obtained from the reused Co TPFPP/np-CTS were more than those from Co TPFPP/nonp-CTS (Table 3). Anyway, there were the similar situation in both catalysts: the C–H bonds of CTS surface would be probably oxidized and then both were gradually changed to black.

Third, the TOFs ( or TON) obtained from the cyclohexane oxidation over Co TPFPP were always higher than those over Co TPFPP/nonp-CTS (Figure 7). This means that, the weak axial coordination(dBE = −1.0 eV) had little contributed to the enhancement of the catalytic activity for cyclohexane oxidation over Co TPFPP/nonp-CTS; and also indicates that, the covalently grafting did not contribute to the increment of the catalytic activity of Co TPFPP, but was benefit to the reuse of Co TPFPP, i.e. Co TPFPP/nonp-CTS could be reused for next catalyzing the oxidation. However, Co TPFPP could not be reused for the next oxidation of cyclohexane (Table 3), due to the irreversible dimerization and the oxidative self-destruction of the cobalt porphyrin.[46] From the viewpoint of coordination strength, the both dBE data evidenced that, the stronger the axial coordination was, the more the catalytic activity of Co TPFPP/np-CTS was promoted.

Fourth, the discussion above shows that, there was the stronger coordination in the CoTPFPP/np-CTS, relative to in the Co TPFPP/nonp-CTS, but the covalently grafting was very similar for the both catalysts. These probably resulted in the bigger dBE values (0.5 and 0.4 eV) of N atoms in the N–C= and N–Co units in Co TPFPP/np-CTS, relative to those values (0.1 and 0.0 eV) in the latter, and further resulted in the larger dBE value (8.6 eV) of cobalt ion in the former, in comparison with that (8.0 eV) of the latter (Table 2). It means that, the cobalt ion of Co TPFPP/np-CTS had more positive charges (or lower electron cloud density) than that of Co TPFPP/nonp-CTS, resulting in the stronger ability to activate $O_2$, showing the highest catalytic activity (Table 3 and Figure 7).

Fifth, before 2-hours reaction time, the catalytic activity of Co TPFPP was the highest, but since then was quickly dropping; however, the activity of Co TPFPP/np-CTS remarkably increased with proceeding of oxidation reaction; while, the activity of Co TPFPP/nonp-CTS basically kept the original level (see the changes of their TOFs in Figure 7). Because the un-immobilized Co TPFPPs could be rapidly dispersed in cyclohexane, forming the independent active sites as much as they could, rapidly activating $O_2$ to oxidize cyclohexane, and obtaining its high TOFs. But, they were rapidly destroyed by $O_2$ in absence of protection by CTS, resulting in quickly dropping of the TOFs. The catalyst, Co TPFPP/np-CTS, relying on the stronger axial coordination between cobalt ion and amino group in itself, however, steadily gave the increasingly TOFs. For Co TPFPP/nonp-CTS, it was not promoted due to the weak axial coordination, thus only maintained the lower catalytic activity level. If it was not true, there were more independent active sites (0.14 At%) on the surface of Co TPFPP/nonp-CTS than those (0.12 At%) on that of Co TPFPP/np-CTS (Figure 1 (a) and (b)); it should showed more highly catalytic activity for the cyclohexane oxidation, but the fact was not true (Figure 7 TOFs).

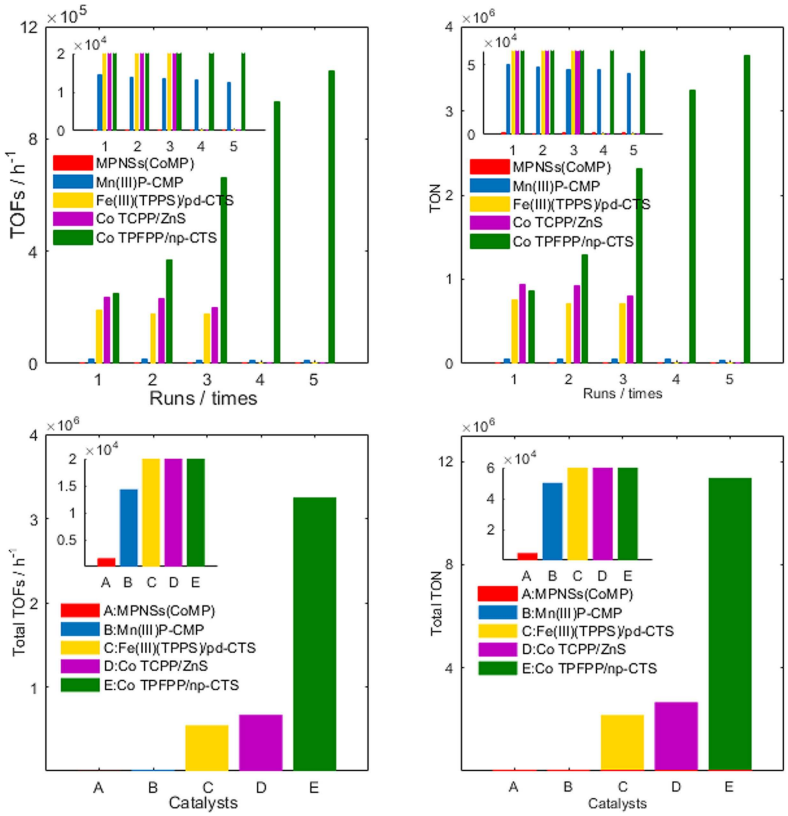


**Figure 8.** Top) The TOF (left) and TON (right) of cyclohexane oxidation over various catalysts reused. Bottom) the total TOF (left) and TON (right) of cyclohexane oxidation over different catalysts.

Sixth, under the ~60 ppm of cobalt loading amount, Co TPFPP/np-CTS could be reused 4 times for the cyclohexane oxidation (Table 3 and Figure 8), which was twice as muchas the recycling ability of the previous catalysts: Co TCPP/ZnS,[17] and Fe(III) TPPS/pd-CTS.[18] For each reuse, it showed the highest catalytic activity (TOF) relative to the two others just mentioned. It is more important that, the total TOFs (TON) of the cyclohexane oxidation catalyzed by Co TPFPP/np-CTS high reached $3.25\times10^{6}$ $h^{-1}$ ($1.14\times10^{7}$). Moreover, the ICP-OES analyses show that the cobalt content (0.0034%) in the fifth-recovered Co TPFPP/np-CTSwas very close to that (0.0035%) of the first-usedcatalyst, which indicates that the Co TPFPP/np-CTS catalyst did not show leaching in cyclohexane. These facts demonstrate that, the covalently grafting had not only an important promotion for the total TOFs (TON), but also the stabilization of np-CTS-immobilized Co TPFPP catalyst for the cyclohexane oxidation.The total TOFs of Co TPFPP/np-CTS was ~5 times as much as those of Co TCPP/ZnS, and Fe(III) TPPS/pd-CTS; ~48 and ~2078 times as much as those of Mn(III) P-CMP,[47] and MPNSs(CoMP).[48]

In summary, it was the axial coordination that tuned high the catalytic activity [TOFs] of Co TPFPP/np-CTS. Obviously, it possessed the highest biomimetic catalytic activity relative to other catalysts in Table 3, and even including two biomimetic catalysts recently reported: Mn(III) P-CMP and MPNSs (CoMP).

## 3. Conclusions

We have successfully prepared a new np-CTS immobilized cobalt porphyrin catalyst and explored the effects of axial coordination, covalently grafting, and nanocavity on the catalytic performances (activity and reusability) of the cobalt porphyrin immobilized on chitosan under the RSM-optimized oxidation conditions: 165.14 °C, 0.8 MPa and 0.98 mg amount of Co TPFPP. Our experimental resultssuggest: 1. Co TPFPP/np-CTS was an excellent biomimetic catalyst with very high activity for oxidizing cyclohexane (total TOFs $3.25\times10^{6}$ $h^{-1}$); 2.The synergism of axially coordination and nanocavity, especially the coordination, mainly enhanced the catalytic activity of Co TPFPP/np-CTS; 3.The covalently grafting action played a decisive role in increasing the total TOFs of the immobilized catalysts, and in reusing of CTS-immobilized Co TPFPP catalysts;4.The weak axial coordination did little effect on the catalytic activity of Co TPFPP/nonp-CTS.

In brief, the Co TPFPP/np-CTS should be an excellent biomimetic catalyst for cyclohexane oxidation at present as far as the TOFs, reusability, yields (KA oil) and especially clean production are concerned. Therefore, Co TPFPP/np-CTS catalyst is promising for using in sustainable green chemical industry.

## Experimental Section

All solvents and reagents, including cobalt tetrakis(pentafluorophenyl)porphyrin, were of commercial grade unless stated otherwise, and purchased from Sigma-Aldrich in China. Powdered chitosan (MW ~$7.7\times10^4$ Da, degree of deacetylation was 90.3%, 4000 mesh) was purchased from JINKE Biochemistry Co Ltd (Zhejiang China). Cyclohexane was analyzed by gas chromatography before use, to ensure it was free of oxidation products.

### Preparation of Nanoporous Chitosan-Grafted Metalloporphyrin Materials

22.5 grams of powdered chitosan were dissolved in 1200 mL (0.6 mol·$L^{-1}$) of diluted acetic acid, with stirring for 6 hours. The resulting colloidal solution was added dropwise to the NaOH solution (10%, m/m), forming white colloid-chitosan microballs (Diameter≈4 mm), which were then immersed in distilled water for 6 hours, afterwards filtered and washed with deionized water until pH=7. The microballs were added to 1500 mL (10%,m/m) of a glutaraldehyde solution for cross-linking for approximately 24 hours, filtered, and thoroughly washed with 3000 mL of deionized water. A portion of the shallow yellow chitosan microballs was dried in a freeze dryer at −57 °C for 50 hours, obtaining yellow nanoporous chitosan microballs, while the other portion was dried in vacuum at 60 °C for 8 hours, obtaining red non-porous chitosan microballs.

20 grams of np-CTS were added to 800 mL ($1.94\times10^{-5}$ mol·$L^{-1}$) of ethylene glycol of Co TPFPP, and the mixture was heated to 100 °C in a microwave oven for 1 hour, with magnetic stirring. The reaction mixture was then cooled down to room temperature and filtrated, and the filter cake was washed with dichloromethane and methanol by using the Soxhlet procedure for 12 hours in each solvent respectively, until the cobalt porphyrin was no longer detected in the extract. Np-CTS grafted Co TPFPP, Co TPFPP/np-CTS was dried in a vacuum pump at 65 °C for 12 hours, and obtained. The blank operation for np-CTS was same as above, but no Co TPFPP was added. Nonp-CTS grafted Co TPFPP, Co TPFPP/nonp-CTS, was also obtained in the same method. The amounts of Co TPFPP grafted per gram of np-CTS and nonp-CTS were $5.91\times10^{-7}$ and $7.95\times10^{-7}$ mol, respectively. These values were determined by using inductively coupled plasma optical emission spectroscopy (ICP-OES).[18]

### Instrumentation

The grafted metalloporphyrin materials were characterized by using the following instruments. Scanning electron microscopy (SEM) and energy dispersive spectra (EDS) were conducted on a S-3400N scanning electron microscope coupled with an energy dispersive analysis detector. Scanning transmission electron microscopy (STEM) was performed by using a Titan ETEM $G^2$ 80-300 scanning transmission electron microscope at an accelerating voltage of 300 kV.The specific Brunauer–Emmet–Teller surface areas ($S_{BET}$),$N_2$ adsorption/desorption isotherms,and Barrett-Joyner-Halenda (BJH) pore-size distribution curves at 77 K were measured with TriStar II 3020 in an ultra-high-purity grade (99.999%) liquid nitrogen bath. UV-Vis spectra were recorded using a Perkin-Elmer L-17 spectrometer. The cobalt content of the immobilized catalyst was measured on Inductively Coupled Plasma Optical Emission Spectrometer (ICP-OES, Optima 2100DV, Perkin Elmer, USA). For ICP-OES, ~0.05 g of catalyst was leached out using conc. $HNO_3$ and final volume was made up to 25 mL by adding distilled water. Fourier-transform infrared (FTIR) spectra were obtained with a resolution of 4 $cm^{-1}$, at room temperature, in KBr media, by using the Perkin-Elmer model 783 FTIR spectrophotometer. The resonance Raman spectra were measured with a RENISHAW inVia-2000 spectrometer equipped with a liquid nitrogen-cooled CCD detector (England Instruments). Excitation wavelengths was 325-nm lines from a Krypton ion laser (Coherent, Innova 90), the Si 520 $cm^{-1}$ Raman peak was used for spectral calibration. X-ray photoelectron spectroscopy (XPS) was performed with an XPS spectrometer (Kratos Ultra Axis DLD) equipped with an Al $K_\alpha$ radiation source, at 150 W, with a pass energy of 40 eV.

### Measurement of Catalytic Performance for the Catalyst Materials

Cyclohexane oxidation over the Co TPFPP/np-CTS was performed under the following general testing procedure: a mixture of certain amount of Co TPFPP/np-CTS catalyst and cyclohexane (200 mL) was sealed in an autoclave reactor equipped with a magnetic stirrer and a frozen ethanol re-condenser at−20 °C. The mixture was stirred and heated to the desired temperature under 0.1 MPa $N_2$. To achieve a desired pressure, $O_2$ was then continuously introduced into the reaction system. The desired pressure was varied from 0.7 to 0.9 MPa; the oxidation reaction was conducted in the temperature range of 160–170 °C, and the catalyst amount of Co TPFPP was used in the range of 0.5 to 1.5 mg. Liquid samples of the oxidation mixture were withdrawn every 30 minutes and quantified by Gas Chromatography Spectrometry (GC) on the Shimadzu GC-16A chromatograph equipped with a 30 m×0.32 mm×0.5 μm FFAP capillary column and a flame ionization detector, using chlorobenzene as the internal standard substance. All of the catalytic cyclohexane oxidations were run for 3.5 hours and terminated, and the catalyst material was separated from the oxidation mixture by filtration, washed in ethanol, air-dried to remove residual oxidation products, and reused for the next oxidation of cyclohexane.

The optimized reaction conditions (reaction temperature, reaction pressure, and amount of catalyst) for cyclohexane oxidation over the Co TPFPP/np-CTS were obtained via RSM (see supplementary materials), and then the next investigation and comparison of the catalytic activities of the three catalysts (Co TPFPP/np-CTS, Co TPFPP/nonp-CTS, and Co TPFPP)were carried out under the optimal reaction conditions.

## Acknowledgements

*This research was supported by the National Natural Science Foundation of China (No. 51363001), the Guangxi Natural Science Foundation (No. 2014GXNSFDA118009), and the Guangxi Scientific and Technological Project (No. 12118008-12-3).*

## Conflict of Interest

The authors declare no conflict of interest.

**Keywords:** cobalt porphyrin · covalently grafting-action and axial coordination · promotion · catalysis · nanocavity

[1] X. Y. Huang, J. T. Groves, *Chem. Rev.* **2018**, *118*, 2491–2553.

[2] F. Schwizer, Y. Okamoto, T. Heinisch, Y. F. Gu, M. M. Pellizzoni, V. Lebrun, R. Reuter, V. Köhler, J. C. Lewis, T. R. Ward, *Chem. Rev.* **2018**, *118*, 142–231
[3] M. M. Pereira, L. D. Dias, Mário J. F. Calvete, *ACS Catal.* **2018**, *8*,10784–10808
[4] F. G. Cantu Reinhard, M. A. Sainna, P. Upadhyay, G. A. Balan, D. Kumar, S. Fornarini, M. E. Crestoni, S. P. de Visser, *Study. Chem. Eur. J.* **2016**, *22*, 18608–18619.
[5] K. Zhang, O. K. Farha, J. T. Hupp, S. T. Nguyen, *ACS Catal.* **2015**, *5*,4859–4866.
[6] X. F. Sheng, H. C. Guo, Y. S. Qin, X. H. Wang, F. S. Wang, *RSC Adv.* **2015**,*5*, 31664–31669.
[7] S. Meng, X. Q. Zou, C. F. Liu, H. P. Ma, N. Zhao, H. Ren, M. J. Jia, J. Liu, G. S. Zhu, *ChemCatChem.* **2016**,*8*, 2393–2400.
[8] V. Christoforidis, D. A. Pantazis, L. L. Bonilla, E. Bletsa, M. Louloudi, Y. Deligiannakis, *J. Catal.* **2016**,*344*, 768–777.
[9] P. K. Das, K. Mittra, A. Dey, *Chem. Commun.* **2014**,*50*, 5218–5220.
[10] G. Huang, R. X. Yuan, Y. Peng, X. F. Chen, S. K. Zhao, S. J. Wei, W. X. Guo, X. Chen, *RSC Adv.* **2016**, *6*, 48571–48579.
[11] P. Battioni, J. P. Renaud, J. F. Bartoli, M. Reina-Artiles, M. Fort, D. Mansuy, *J. Am. Chem. Soc.* **1988**,*110*,8462–8470.
[12] P. N. Balasubramanian, E. S. Schmidt, T. C. Bruice, *J. Am. Chem. Soc.* **1987**,*109*,7865–7873.
[13] T. Dewa, M. Satoh, J. Komiyama, *Macromol. Chem. Phys.* **1994**,*195*, 2917–2929.
[14] Y. Sun, X. B. Hu, H. R. Li, A. F. Jalbout, *J. Phys. Chem. C.* **2009**,*113*,14316–14323.
[15] W. J. Zhang, Y. Wang, Y. Leng, P. B. Zhang, J. Zhang, P. P. Jiang, *Catal. Sci. Technol.* **2016**,*6*, 5848–5855.
[16] C. M. Krest, A. Silakov, J. Rittle, T. H. Yosca, E. L. Onderko, J. C. Calixto, M. T. Green, *Nat. Chem.* **2015**,*7*, 696–702.
[17] G. Huang, W. L. Wang, X. X. Ning, Y. Liu, S. K. Zhao, Y. A. Guo, H. Zhou, *Ind. Eng. Chem. Res.* **2016**,*55*, 2959–2969.
[18] G. Huang, Y. Liu, J. L. Cai, X. F. Chen, S. K. Zhao, Y. A. Guo, S. J. Wei, X. Li, *Appl. Surf. Sci.* **2017**, *402*, 436–443.
[19] Q. Sun, Z. F. Dai, X. J. Meng, F. S. Xiao, *Chem. Soc. Rev.* **2015**,*44*, 6018–6034.
[20] Y. J. Li, B. S. Sun, Y. R. Zhou, W. J. Yang, *Appl. Organomet. Chem.* **2016**,*31*, 1–7.
[21] A. Modak, J. Mondal, A. Bhaumik, *Appl. Catal. A* **2013**, *459*, 41–51.
[22] I. Tabushi, N. Koga, *J. Am. Chem. Soc.* **1979**,*101*,6456–6458.
[23] D. H. R. Barton, *Tetrahedron.* **1998**,*54*, 5805–5817.
[24] U. Schuchardt, M. J. D. M. Jannini, D. T. Richens, M. C. Guerreiro, E. V. Spinace, *Tetrahedron.* **2001**, *57*,2685–2688.
[25] P. E. Jr. Ellis, J. E. Lyons, *J. Chem. Soc. Chem. Commun.* **1989**,1315–1316.
[26] S. Evans, J. R. Lindsay Smith, *J. Chem. Soc.Perkin Trans.* **2001**,*2*,174–180.
[27] X. Guo, D. H. Shen, Y. Y. Li, M. Tian, Q. Liu, C. C. Guo, Z. G. Liu, *J. Mol. Catal. A* **2011**,*351*, 174–178.
[28] Z. Feng, Y. J. Xie, F. Hao, P. L. Liu, H. A. Luo, *RSC Adv.* **2015**, *5*, 101593–101598.
[29] X. P. Guo, D. Yang, C. C. Zuo, Z. J. Peng, C. S. Li, S. J. Zhang, *Ind. Eng. Chem. Res.* **2017**,*56*, 5860–5871.
[30] N. F. Sulaiman, W. A. W. A. Bakar, R. Ali, *Renewable Energy* **2017**,*113*, 697–705.
[31] M. E. Alea-Reyes, O. Penon, P. G. Calavia, M. J. Marín, D. A. Russe, L. Pérez-García, *J. Colloid Interface Sci.* **2018**, *521*, 81–90.
[32] R. X. Wang, B. J. Gao, W. Z. Jiao, *Appl. Surf. Sci.* **2009**,*255*, 4109–4113.
[33] D. Samaroo, C. E. Soll, L. J. Todaro, C. M. Drain, *Org. Lett.* **2006**,*8*, 4985–4988.
[34] K. D. Dimzon, T. P. Knepper, *Inter. J. Biol. Macr.* **2015**, *72*, 939–945.
[35] H. W. Hu, J. H. Xin, H. Hu, A. Chan, L. He, *Carbohydr. Polym.* **2013**,*91*, 305–313.
[36] M. L. Duarte, M. C. Ferreira, M. R. Marvao, J. Rocha, *Int. J. Biol. Macromol.* **2002**,*31*,1–8.
[37] L. J. Boucher, J. J. Katz, *J. Am. Chem. Soc.* **1967**, *89*,1340–1345.
[38] J. Zawadzki, H. Kaczmarek, *Carbohydr. Polym.* **2010**, *80*, 394–400.
[39] N. Bizaia, E. H. D. Faria, G. P. Ricci, P. S. Calefi, E. J. Nassar, K. A. D. F. Castro, S. Nakagaki, K. J. Ciuffi, R. Trujillano, M. A. Vicente, A. Gil, S. A. Korili, *ACS Appl. Mater. Interfaces* **2009**, *1*,2667–2678.
[40] S. N. Terekhov, S. G. Kruglik, V. L. Malinovskii, V. A. Galievsky, V. S. Chirvony, P.-Y. Turpin, *J. Raman Spectrosc.* **2003**, *34*, 868–881.
[41] N. Blom, J. Odo, K. Nakamoto, *J. Phys. Chem.* **1986**, *90*, 2847–2852.
[42] J. M. Burke, J. R. Kincaid, T. G. Spiro, *J. Am. Chem. Soc.* **1978**, *100*, 6077–6083.
[43] K. S. Lokesh, M. D. Keersmaecker, A. Elia, D. Depla, P. Dubruel, P. Vandenabeele, S. V. Vlierberghe, A. Adriaens, *Corros. Sci.* **2012**,*62*, 73–82.
[44] S. Z. Hu, *Inorg. Chem.* **1993**,*32*, 1081–1085.
[45] E. A. Dierks, S. Z. Hu, K. M. Vogel, A. E. Yu, T. G. Spiro, J. N. Burstyn, *J. Am. Chem. Soc.* **1997**,*119*,7316–7323.
[46] J. Haber, L. Matachowski, K. Pamin, J. Połtowicz, *Catal. Today* **2004**,*91–92*,195–198.
[47] Y. Li, C. Liu, W. Yang, *New J. Chem.* **2017**, *41*, 8214–8221.
[48] P. Zhao, M. Liu, M. Zheng, S. Jin, D. Tang, J. Lin, Y. Ma, J. Chen, H. Liu, *J. Nanosci. Nanotechnol.* **2016**, *16*, 9843–9850.

Manuscript received: November 26, 2018
Revised manuscript received: December 16, 2018
Version of record online: ■■, ■■■